JOURNAL OF
HYDRO-METEOROLOGY

Research Article

Application GIS and remote sensing methods to assess the change in land surface temperature in Ba Ria - Vung Tau province, Vietnam

Nguyen Hai Au[1,2*]

[1] Institute for Environment and Resources; haiauvtn@gmail.com
[2] Vietnam National University Ho Chi Minh City; haiauvtn@gmail.com

*Corresponding author: haiauvtn@gmail.com; Tel.: +84–989115280

Received: 14 March 2024; Accepted: 17 April 2024; Published: 25 June 2024

Abstract: Ba Ria-Vung Tau province is situated in the Southern main economic area with rapid urbanization, industry, and modernization. The expansion of impermeable land cover has grown significantly in response to climate change and global warming, which have resulted in higher surface temperatures in the province in recent years. This study provides an assessment of the impact of increased temperature in Ba Ria - Vung Tau province based on surface temperature values extracted from thermal infrared Landsat image data during the period 2010-2021. The variety of land cover tends to influence the properties of land surface temperature reported by satellite sensing sensors. The results show that the heat island activity is strong, with a decreasing trend from urban to peri-urban areas. The surface temperatures above 30-40^{o}C accounted for just 5% of the study area in 2010, but the rate doubled by 2021. Typical areas with an increase in surface temperature due to the rapid urbanization include Vung Tau city, Ba Ria city, Long Dien district, and Phu My town. This demonstrates that the changes in land cover is a factor contributing to the increase in land surface temperature in the area.

Keywords: Remote sensing; Surface temperature; Land cover change.

1. Introduction

In parallel with population growth, urbanization and industrialization have accelerated rapidly. This has resulted in fast changes in land use which affected the vegetation cover on the Earth surface tremendously. Particularly, this affects the distribution of solar radiation, leading to an increase in atmospheric temperature, especially in urbanizing areas with hotter temperatures than rural areas [1, 2]. Many studies on the effects of land cover change on atmospheric dynamics and climate change have been conducted across the world. The expansion of building causes the shrinkage of green areas, which causes a rise in the Earth's surface temperature [3–6], which may be detected by measuring the emissivity of vegetation and soil.

With the advanced technologies of remote sensing, satellite images are now the best option for analyzing surface cover changes and swiftly collecting data. In particular, Landsat images have been widely utilized in numerous studies to monitor local and global temperature changes. Land cover is one of the primary elements influencing surface temperature as shown in remote sensing images. According to previous studies, the surface temperatures of different land uses have significant differences [6]. Temperatures increase in areas influenced by anthropogenic activities and construction facilities, while being low in areas with vegetation [1]. Remote sensing offers high-resolution data with consistent Earth surface coverage, making it easy to

extract information from satellite data [7]. The combined use of remote sensing with GIS is effective in visualizing extracted information and monitoring land use changes. Climate change and surface changes have led to extensive assessments of land surface temperature changes in various global regions. Studies in Indonesia [3], Nigeria [5], Iran [8], India [9], Egypt [7] evaluated surface temperatures using heat bands in Landsat data using remote sensing and GIS. According to research findings, there is a considerable reduction in the amount of vegetation due to urban expansion, which raises surface temperatures.

In recent years, many Vietnamese researchers have paid their attention and interest in analyzing surface temperature fluctuations in the context of global climate change [10–13]. The study [10] claimed that pressure from the processes of industrialization, modernization, and urbanization in Ho Chi Minh (HCM) city is the main factor of higher surface temperatures and a robust urban heat island phenomenon. Similarly, studies in HCM [13], Binh Duong [11], and Hai Phong [12] analyzed land surface temperature changes based on impermeable surfaces in land cover and thermal infrared images using Landsat imagery.

Ba Ria - Vung Tau (BR-VT) province is located in the Southeast and serves as the entrance to the East Sea of provinces in the region with significant expansion of urbanization, industrialization, and modernization. The average amount of sunlight hours ranges from 170 hours/month in September to 299 hours/month in April. The change in average temperature in months (2015-2021) is around 0.6-2ºC compared to the average annual temperature.

This study aims to determine land use changes through classification and land surface temperature fluctuations in Ba Ria - Vung Tau province using Landsat data through the integration of remote sensing and GIS. In the context of climate change and global warming, this research can also be helpful in regulating and assisting decision-makers with a visual picture of high-temperature areas and urban construction development.

2. Methods and data

2.1. Study area

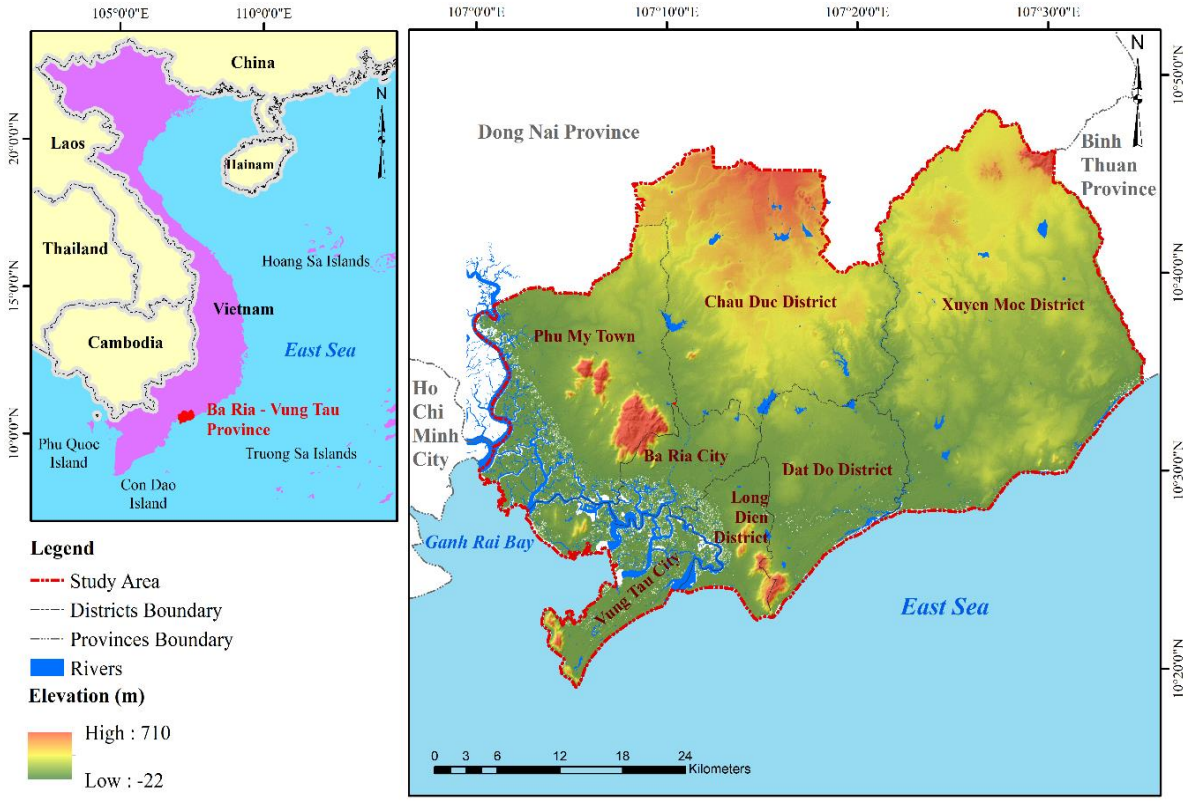

Figure 1. Location of the study area.

BR-VT province is located in the Southern key economic region, at the entrance to the East Sea of the provinces in the Southeast region, with rapid development, with rapid development of urbanization, industry, and modernization including changes in land use and temperature. This study was conducted throughout the province, including Vung Tau and Ba Ria cities, Phu My town, Long Dien district, Dat Do district, and Xuyen Moc district have an area of approximately 1473 km^2 (Figure 1). located in the tropical monsoon zone, with two distinct seasons and high temperatures. The area of urban and concrete land has increased rapidly, leading to rising surface temperatures, and marking urban heat island activity in recent years. This has been contributing a part to the global warming leading to climate change. BR-VT province has abundant radiation sources from sunlight. The study area's average temperature is 28.01°C.

2.2. Data

In the study, the data used is Landsat 7 images (for the period before February 2013) and Landsat 8 images of BR-VT province including 7 districts, cities and town collected from the United States Geological Survey at the earthexplorer.usgs.gov website [14]. The Landsat image data collected has been modified to correct terrain elevation deformation. It was collected twice (16 March 2010; 24 March 2016 and 06 March 2021) during the dry season (December to April of the following year), images have high quality and negligible cloud influence (cloud ratio < 1%), coordinates UTM-WGS-84 zone 48 North (Table 1).

Table 1. Detailed information on Landsat satellite.

No.	Satellite	Acquisition time	Spatial resolution (m)
1	Landsat 7	16/03/2010	30
2	Landsat 8	24/03/2016	30
3	Landsat 8	06/03/2021	30

Landsat 7 is equipped with an enhanced thematic mapper plus (ETM+) map sensor with 185 kilometers scanning range. The TM sensor contains 7 bands for recording electromagnetic spectrum reflections or radiation emitted from the earth's surface and 1 panchromatic band (Table 2) [15].

Landsat 8 improves on previous generations in terms of performance and dependability by carrying two sensors: Operational land imager (OLI) and thermal infrared sensor (TIRS). The scanning band width is 190 kilometers. Landsat 8 picture includes 11 spectral bands (9 shortwave bands and 2 longwave thermal bands) (Table 2) [16]. These three images provide seasonal detail of the Earth's surface with a spatial resolution of 30 m.

Table 2. Landsat satellite specifications [16].

Landsat 7 ETM+ Bands				**Landsat 8 OLI and TIRS Bands**			
Bands		Wavelength (μm)	Resolution (m)	Bands		Wavelength (μm)	Resolution (m)
				Band 1	Coastal/ Aerosol	0.435-0.451	30
Band 1	Blue	0.441-0.514	30	Band 2	Blue	0.452-0.512	30
Band 2	Green	0.519-0.601	30	Band 3	Green	0.533-0.590	30
Band 3	Red	0.631-0.692	30	Band 4	Red	0.636-0.673	30
Band 4	NIR	0.772-0.898	30	Band 5	NIR	0.851-0.879	30
Band 5	SWIR-1	1.547-1.749	30	Band 6	SWIR-1	1.566-1.651	30
Band 6	TIR	10.31-12.36	60	Band 7	SWIR-2	2.107-2.294	30
Band 7	SWIR-2	2.064-2.345	30	Band 8	Pan	0.503-0.676	15
Band 8	Pan	0.515-0.896	15	Band 9	Cirrus	1.363-1.384	30
				Band 10	TIR-1	10.60-11.19	100
				Band 11	TIR-2	11.50-12.51	100
NIR - Near Infrared SWIR - Shortwave Infrared				Pan - Panchromatic TIR - Thermal Infrared			

2.3. Methods

2.3.1. Remote sensing images interpretation

Atmospheric correction will aid in the elimination of confounding variables that alter the image band's reflectance value taken by satellite sensors, boosting the dependability of the analysis results. The procedure for performing land surface temperature calculations and the methods used are shown in Figure 2.

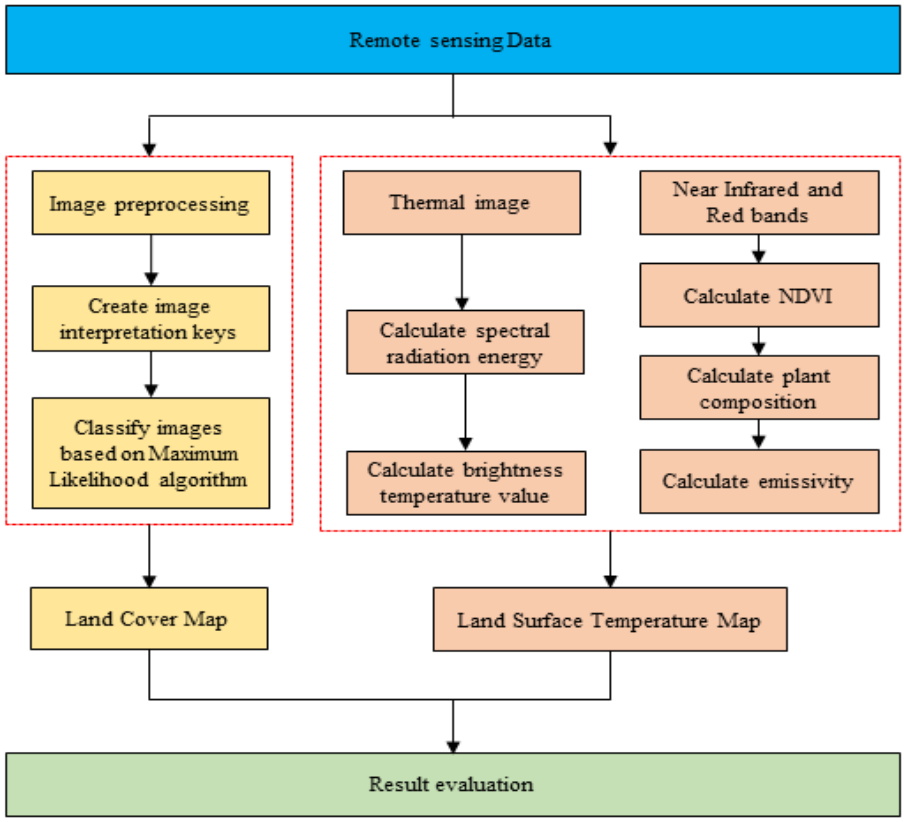

Figure 2. Methodology for land surface temperature assessment.

2.3.2. Land surface temperature from Landsat 8 image data

This study uses the emissivity from normalized difference vegetation index approach to calculate land surface temperature using Landsat 8 image data.

Converting numerical values to spectral radiant energy values: Landsat satellite image data will be modified for radiation after being captured, transforming numerical values to spectral reflected energy values. Because there is no link between the spectral radiation value and Landsat 8 image data, so it should be calculated directly according to the following formula [16, 17]:

$$L_\lambda = M_L \times Q_{cal} + A_L \quad (1)$$

where L_λ is the spectral radiance; M_L is the band-specific multiplicative rescaling factor from the Landsat 8 image metadata file (M_L = 0.0003342); Q_{cal} is the quantized and calibrated standard product pixel values; AL is the band-specific additive rescaling factor from the Landsat 8 image metadata file (AL = 0.1).

Conversion to Top of Atmosphere Brightness Temperature: Using the thermal constants in the metadata file, thermal band data can be converted from spectral radiance to top of atmospheric brightness temperature [10].

$$T_b = \frac{K_2}{\ln\left(\frac{K_1}{L_\lambda} + 1\right)} - 273{,}15 \quad (2)$$

where T_b is the top of atmosphere brightness temperature; L_λ is TOA spectral radiance; K_1, K_2 are the band-specific thermal conversion constant from the Landsat 8 image metadata file (K_1 = 774.88; K_2 = 1321.07).

Normalized difference vegetation index (NDVI): NDVI is a typical technique that uses reflectance measurements at red and near-infrared wavelengths to determine the quality of terrestrial green vegetation. Use the following formula to determine the NDVI value [18]:

$$NDVI = \frac{NIR - RED}{NIR + RED} \quad (3)$$

where NDVI is the normalized Difference Vegetation Index; NIR is the near-infrared band of Landsat 8 remote sensing image; RED is the red band of Landsat 8 remote sensing image.

Proportion of Vegetation: The proportion of vegetation is calculated according to the formula [18]:

$$P_v = \left(\frac{NDVI - NDVI_{min}}{NDVI_{max} - NDVI_{min}}\right)^2 \quad (4)$$

where P_v is the proportion of vegetation; $NDVI_{min}$ and $NDVI_{max}$ are values range from -1 to 1.

Surface emissivity: The emissivity of natural surfaces varies due to different land cover characteristics, such as the distinction between fields, urban areas, and vacant land [10, 19]. Surface emissivity (ε) is calculated based on the following formula [10, 18, 19]:

$$\varepsilon = mP_v + n \quad (5)$$

where $m = \varepsilon_v - \varepsilon_s - (1 - \varepsilon_s)F\varepsilon_v$; $n = \varepsilon_s(1 + \varepsilon_s)F\varepsilon_v$

where ε_v and ε_s are the surface emissivities of the vegetated surfaces and vacant land, respectively. The reference values for ε_v and ε_s are 0.99 and 0.97, respectively [19]. And F is the shape index, assuming a different geometric distribution and F = 0.55 [19, 20]. Therefore, the formula is represented precisely as follows:

$$\varepsilon = 0.004 \times P_v + 0.986 \quad (6)$$

where ε is the surface emissivity; P_v is the proportion of vegetation values.

Land surface temperature (LST): is the radiation temperature calculated from the brightness temperature, wavelength of emitted radiation, and land surface emissivity using the following formula [3, 16, 19]:

$$T_S = \frac{T_b}{1 + \left(\lambda \frac{T_b}{\rho}\right) Ln(\varepsilon)} \quad (7)$$

where T_S is the land surface temperature; T_b is the top of atmosphere brightness temperature; λ is the wavelength of emitted radiation; ε is the surface emissivity.

The wavelength of the radiated heat band $\rho = \frac{hc}{\sigma} = 1{,}4388 \times 10^{-2}\,mK = 14388\,\mu mK$

2.3.3. Land surface temperature from Landsat 7 image data

Perform calculations to convert pixel values from numerical values to spectral radiant values according to the formula [15]:

$$L_\lambda = \left(\frac{L_{max} - L_{min}}{Q_{cal\,max} - Q_{cal\,min}}\right) \times (Q_{cal} - Q_{cal\,min}) + L_{min} \quad (8)$$

where L_λ is the spectral radiance; Q_{cal} is the quantized and calibrated standard product pixel values; L_{max}, L_{min} are the spectral radiation value is calculated corresponding to each low gain and high gain state (Table 3).

Table 3. L_{max}, L_{min} values for LANDSAT 7 thermal images.

Band	Satellite	Lmax	Lmin
6.1	LANDSAT 7 /ETM+ High gain	17.04	0
6.2	LANDSAT 7 /ETM+ Low gain	12.65	3.2

Convert the value of spectral radiance to temperature: The image is converted from spectral radiance values to physical variables. The satellite's effective temperature (black-body temperature) and conversion using the Planck physics formula [21]:

$$T_S = \frac{K_2}{Ln\left(\frac{K_1}{L_\lambda}+1\right)} \quad (9)$$

where T_s is the land surface temperature; L_λ is the spectral radiance; K_1, K_2 are the correction factor is provided in the Landsat 7 image metadata file (Table 4).

Table 4. K_1, K_2 values for LANDSAT 7 thermal images.

Band	Satellite	K1	K2
6.1	LANDSAT 7 /ETM+ High gain	666.09	1282.71
6.1	LANDSAT 7 /ETM+ Low gain	666.09	1282.71

2.3.4. Evaluate accuracy after classification

The Kappa index (K) is often used to evaluate the dependability of remote sensing image classification maps [9], which is calculated according to the following formula:

$$K = \frac{(T-E)}{(1-E)} \quad (10)$$

where T is an overall accuracy by digital matrix; E is the quantity representing the expectation of predictable classification accuracy.

The following table 5 illustrates the correlation between the accuracy of the classification map and the range of the Kappa coefficient.

Table 5. Ranges for the Kappa Coefficient [9].

Kappa Coefficient	Classification
< 0.4	Poor
0.41 - 0.60	Moderate
0.61 - 0.75	Good
0.76 - 0.80	Excellent
> 0.81	Almost perfect

3. Results and discursion

3.1. Component parameter

To determine the surface temperature in Ba Ria - Vung Tau province in 2010-2021, the collected remote sensing data is processed and calculated, respectively: Spectral Radiation values; Surface emissivity; Brightness temperature; NDVI index; Value of proportion of vegetation. These values are calculated from Landsat 7 and Landsat 8 images, using the Raster Calculator tool of ArcMap 10.4.1 software (shown in Figure A1, A2, A3 in the Appendix section).

3.2. Land cover classification

The land cover classification map illustrates that BR-VT province has many types of cover, including construction areas, residential areas, traffic areas (impervious surfaces); vacant land; fields, forests, plantations (vegetation), and networks of reservoirs and rivers (Figure 3). From 2010 to 2021, the impervious surface cover in Phu My town, Ba Ria and Vung Tau cities and Long Dien district increased significantly, rising from 596.22 km^2 to 680.58 km^2. Meanwhile, the area of vacant land and vegetation tends to decrease (Table 6).

The classification results in 2010, 2016 and 2021 both have Kappa coefficients above 0.8 and overall accuracy above 90% (Table 7) according to the range of the Kappa coefficient in Table 5.

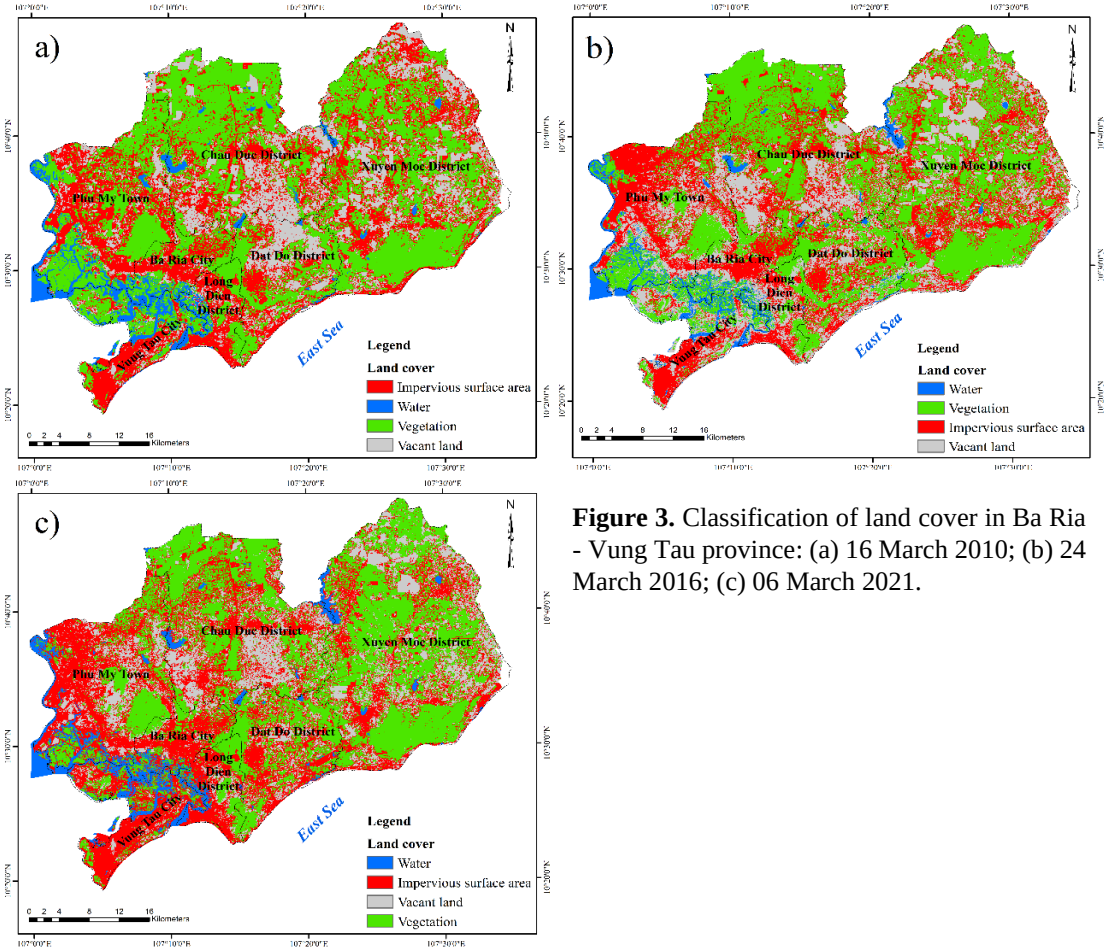

Figure 3. Classification of land cover in Ba Ria - Vung Tau province: (a) 16 March 2010; (b) 24 March 2016; (c) 06 March 2021.

Table 6. Area of land cover in Ba Ria - Vung Tau province.

Types of land cover	16 March 2010		24 March 2016		06 March 2021	
	Area (km^2)	%	Area (km^2)	%	Area (km^2)	%
Impervious surface area	596.22	17.547%	57.23	16.843%	680.58	20.071%
Vacant land	373.99	11.006%	46.85	13.788%	368.60	10.870 %
Vegetation	841.86	24.776%	79.22	23.315%	763.12	22.505 %
Water	94.27	2.774%	7.78	2.289%	94.65	2.791 %

Table 7. Classification accuracy.

Accuracy	2010	2016	2021
Overall Accuracy	97.55%	98.38%	98.57%
Kappa Coefficient	0.9658	0.9773	0.9805

3.2. Land surface temperature

The results of NDVI on 16 March 2010 (Figure 4a); 24 March 2016 (Figure 4b) and 06 March 2021 (Figure 4c) demonstrate that areas with low NDVI values are located mostly in

hydro-system objects, including the Thi Vai River, Dinh River, Ray River, system of rivers, small streams, and lakes in BR-VT province. Low to medium NDVI values are seen in residential areas, construction works, and vacant land. Areas with forests and trees are places with medium to high NDVI values.

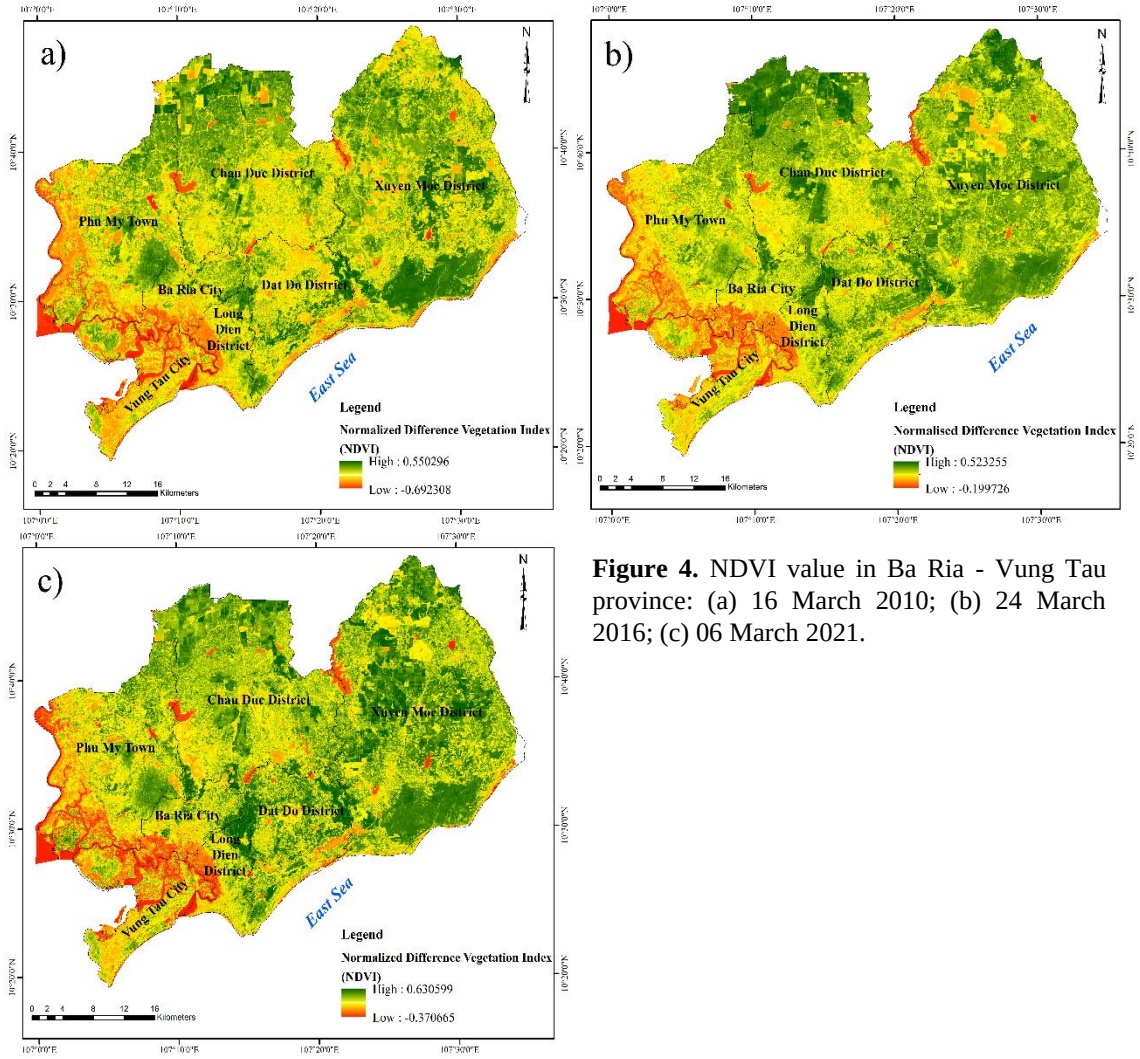

Figure 4. NDVI value in Ba Ria - Vung Tau province: (a) 16 March 2010; (b) 24 March 2016; (c) 06 March 2021.

From the results of analyzing remote sensing images, the area and surface temperature distribution in Ba Ria - Vung Tau province have been determined during the dry season on 16 March 2010; 24 March 2016 and 06 March 2021.

Table 8. Area of temperature levels in Ba Ria - Vung Tau province.

Temperature levels	**16 March 2010**		**24 March 2016**		**06 March 2021**	
	Area (km^2)	%	Area (km^2)	%	Area (km^2)	%
< 24	213.24	11.18	21.95	1.15	0.04	0.0021
24 - 27	769.89	40.38	240.49	12.61	224.13	11.75
27 - 30	726.33	38.09	589.68	30.93	472.94	24.80
30 - 33	190.13	9.97	693.24	36.36	819.45	42.98
33- 37	7.08	0.37	340.41	17.85	380.60	19.96
> 37	0.000616	0.000032	20.94	1.10	9.55	0.50

The surface temperature map shows that in 2010, areas with high temperatures above 30°C only accounted for 10.35% of the area (197.21 km^2); the majority of the areas had temperatures below 30°C, accounting for 1,709.46 km^2 (89.65% area) (Figure 6a). Surface temperature map reveal that the study area has a substantial temperature change by 2016 and 2021. Areas with temperatures below 30°C only account for 44.96% and 36.56% of the area, respectively.

Whereas areas with temperatures over 30°C increased five times and six times compared to 2010, accounting for 55.31% and 63.44% of the area, respectively (Figures 6b, 6c).

Surface temperatures rise in regions with poor vegetation, such as construction areas, as well as high mountain areas exposed to sunshine. The results show that temperatures exceeding 37°C in BR-VT province tend to steadily rise during the dry season. According to Table 8 and Figure 5, the image analysis results in 2010 almost did not reveal a temperature above 37°C, but this temperature existed with an area of 20.94 km^2 by 2016 and 9.55 km^2 by 2021. In contrast, areas with temperatures below 24°C tend to decrease sharply in the dry season, from 213.24 km^2 in 2010 to 21.95 km^2 in 2016 and 0.04 km^2 in 2021. Temperatures of 24-30°C are expected to fall from 1,496.22 km^2 to 697.07 km^2 between 2010 and 2021. While the temperature level from 30 to 37°C gradually increases, the area increased from 197.21 km^2 in 2010 to 1,054.59 km^2 and 1,200.05 km^2 in 2016 and 2021, respectively. The majority of the area is concentrated in Ba Ria and Vung Tau cities, Long Dien district, Phu My town. The Xuyen Moc and Dat Do districts also have an increase in heat, but not much, mainly coming from the formation of many housing projects for residents or coastal tourism regions.

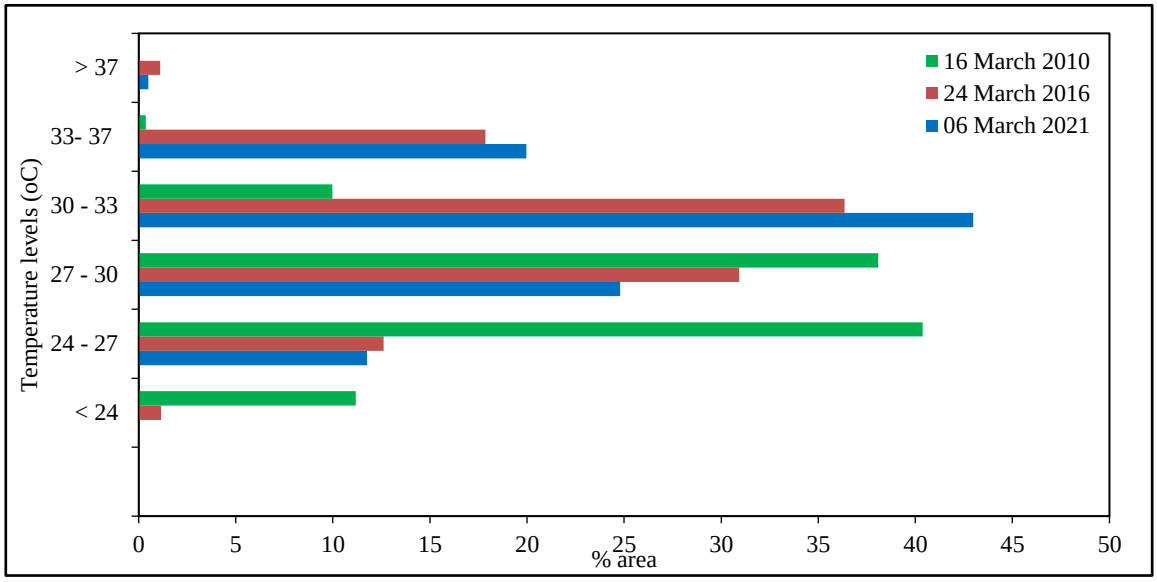

Figure 5. Comparison chart of land surface temperature analysis results.

From the results of land surface temperature, NDVI, and the land cover classification maps of the study area from 2010 to 2021, it shows that vegetation has definitely declined in most districts in the province within 11 years (except Chau Duc and Xuyen Moc districts). The reason is that since 2010, the area's population growth rate has expanded significantly along with the growth of the economy, with the formation of many factories, enterprises, or industrial zones, leading to a large demand for human resources and a large amount of labor. This results in a strong trend of industrialization, urbanization, and tourism services in coastal districts and cities, causing the vegetation area to be converted to residential land and construction land.

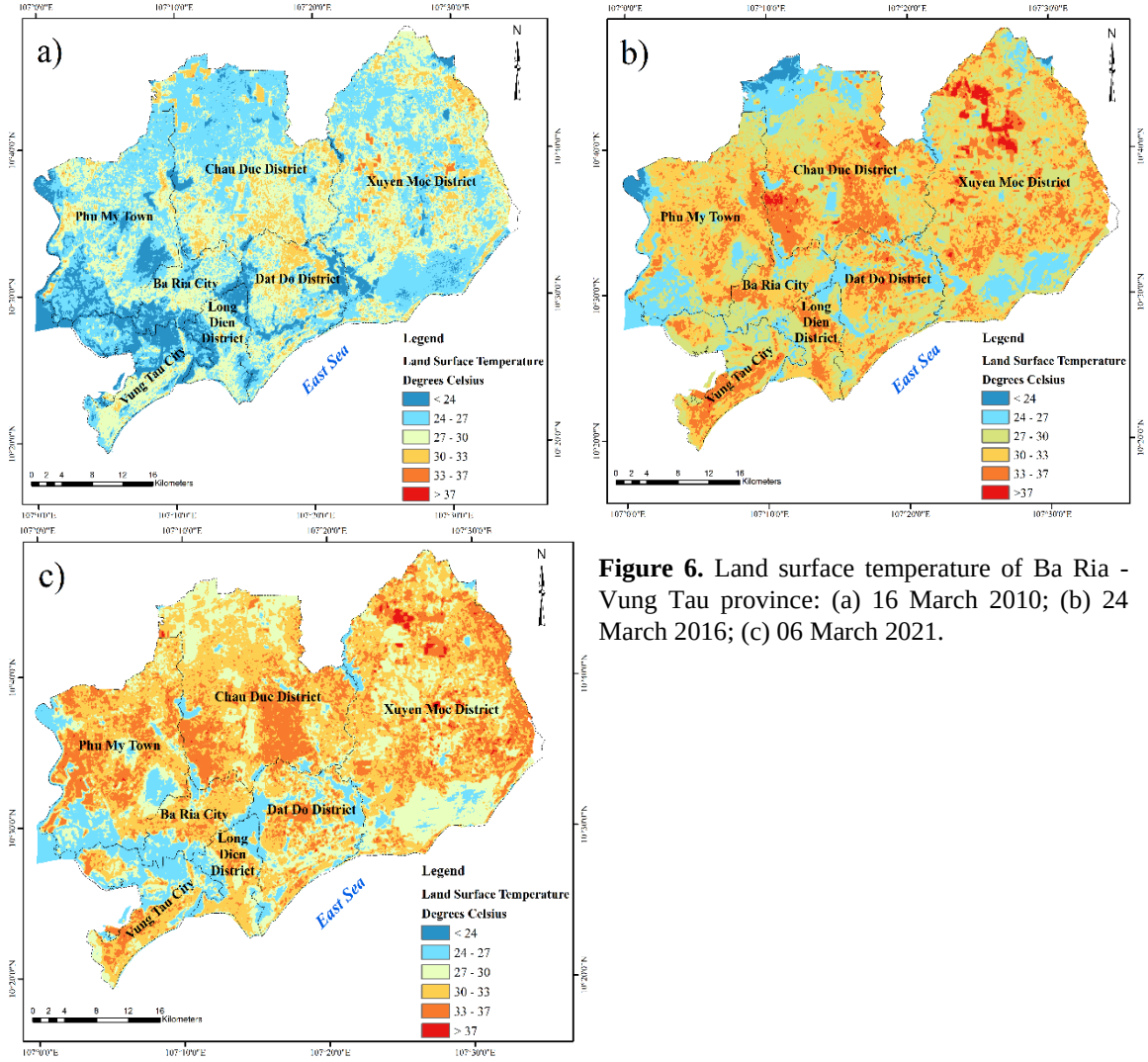

Figure 6. Land surface temperature of Ba Ria - Vung Tau province: (a) 16 March 2010; (b) 24 March 2016; (c) 06 March 2021.

4. Conclusion

This study used Landsat images taken during the dry season to classify surface cover and survey surface temperature by estimating Normalised Difference Vegetation Index (NDVI).

The study's findings indicate that there was a notable increase in the BR-VT area's surface temperature between 2010 and 2021. In particular, in the dry season of 2021, the majority of the study region has a temperature of roughly 30-37^{o}C, a sixfold increase over 2010, concentrated in building zones, residential areas, roadways (impervious surfaces), and vacant land. Meanwhile, compared to 2010, areas with fields, forests, plantations (vegetation), and networks of reservoirs and rivers with temperatures ranging from 24 to 30^{o}C account for only 36.55% of the area.

According to these findings, the land surface temperature in BR-VT province has fluctuated significantly over the years. At the same time, it demonstrates that vegetation cover and activity by humans have a significantly affect the surface temperature in the area. The study provides to giving information to assist managers in taking suitable actions in sustainable urban planning and development, therefore reducing the impact of rising surface temperatures on the urban environment in the context of climate change.

Author contribution statement: Conceptualization, methodology, analyzed and interpreted the data, writing - review, editing and project administration: N.H.A.

Acknowledgements: This research was funded by Vietnam National University Ho Chi Minh City (VNU-HCM) under grant number 562-2022-24-01.

Competing interest statement: The author declare no conflict of interest.

References

1. Hu, W.; Zhou, W.; He, H. The effect of land-use intensity on surface temperature in the Dongting Lake area, China. *Adv. Meteorol.* **2015**, 1–11.
2. Bokaie, M.; Zarkesh, M.K.; Arasteh, P.D.; Hosseini, A. Assessment of urban heat island based on the relationship between land surface temperature and land use/ land cover in Tehran. *Sustainable Cities Soc.* **2016**, *23*, 94–104.
3. Himayah, S.; Ridwana, R.; Ismail, A. Land surface temperature analysis based on land cover variations using satellite imagery. *IOP Conf. Ser.: Earth Environ. Sci.* **2020**, *500(1)*, 012019.
4. Jiang, J.; Tian, G. Analysis of the impact of land use/land cover change on land surface temperature with remote sensing. *Procedia Environ. Sci.* **2010**, *2*, 571–575.
5. Igun, E.; Williams, M. Impact of urban land cover change on land surface temperature. *Global J. Environ. Sci. Manage.* **2018**, *4(1)*, 47–58.
6. Kayet, N.; Pathak, K.; Chakrabarty, A.; Sahoo S. Spatial impact of land use/land cover change on surface temperature distribution in Saranda Forest, Jharkhand. *Model. Earth Syst. Environ.* **2016**, *2(3)*, 1–10.
7. Mohamed, A.; Bernard, A.E. Application of remote sensing techniques and geographic information systems to analyze land surface temperature in response to land use/land cover change in greater Cairo region, Egypt. *J. Geogr Inf. Syst.* **2018**, *10*, 57–88.
8. Mehdi, B.; Mirmasoud, K.Z.; Peyman, Daneshkar A.; Ali, H. assessment of urban heat island based on the relationship between land surface temperature and land use/land cover in Tehran. *Sustainable Cities Soc.* **2016**, *23*, 94–104.
9. Shivakumar, B.R.; Rajashekararadhya, S.V. An investigation on land cover mapping capability of classical and fuzzy based maximum likelihood classifiers. *Int. J. Eng. Technol.* **2018**, *7(2)*, 939–947.
10. Huy, N.A.; Trang, N.T.D.; Nguyen, N.T.T; Trong, T.V.; Son, T.V. Application of remote sensing of Ho Chi Minh city's surface temparature in period 2016–2020. *VN J. Hydrometeorol.* **2021**, *729(9)*, 29–39.
11. Tuyet, N.H.A.; Than, N.H. Application of remote sensing to assess the variation of land surface temperature in Dau Tieng District, Binh Duong province in the context of Climate change in the phase of 2004-2019. Proceeding of Earth and environmental sciences, **2019**, 357–360.
12. Anh, L.V.; Tuan, T.A. Estimation of land surface temperature using emissivity calculated from normalized difference vegetation index. *VN J. Earth Sci.* **2014**, *36(2)*, 184–192.
13. Van, T.T; Bao, H.D.X. Study of the impact of urban development on surface temperature using remote sensing in Ho Chi Minh City, Southern Vietnam. *Geogr. Res.* **2010**, *48(1)*, 86–96.
14. United States Geological Survey. Online available: earthexplorer.usgs.gov.
15. Department of the Interior U.S. Geological survey 2019 Landsat 7 (L7) data users handbook, USA.
16. Department of the Interior U.S. Geological survey 2019 Landsat 8 (L8) data users handbook, USA.
17. LANDSAT Conversion to Radiance. Reflectance and at-Salittite brightness temperature (NASA).
18. Carlson, T.N.; Ripley, D.A. On the relation between NDVI, fractional vegetation cover, and leaf area index. *Remote Sens. Environ.* **1997**, *62(3)*, 241–252.
19. Vo, M.Q; Varnakovida, P.; Iabchoon, S.; Nguyen, D.T.H.; Nguyen, C.T. Analysis of factors affecting urban heat island phenomenon in Bangkok metropolitan area,

Thailand. *VNU J. Sci.: Earth Environ. Sci.* **2019**, *35(1)*, 53–62.
20. Sobrino, J.A.; Jiménez-Muñoz, J.C.; Paolini, L. Land surface temperature retrieval from LANDSAT TM 5. *Remote Sens. Environ.* **2004**, *90(4)*, 434–440.
21. Nugraha, A.S.A.; Gunawan, T.; Kamal, M. Comparison of land surface temperature derived from Landsat 7 ETM+ and Landsat 8 OLI/TIRS for drought monitoring. *IOP Conf. Ser.: Earth Environ. Sci.* **2019**, *313(1)*, 012041.

Appendix

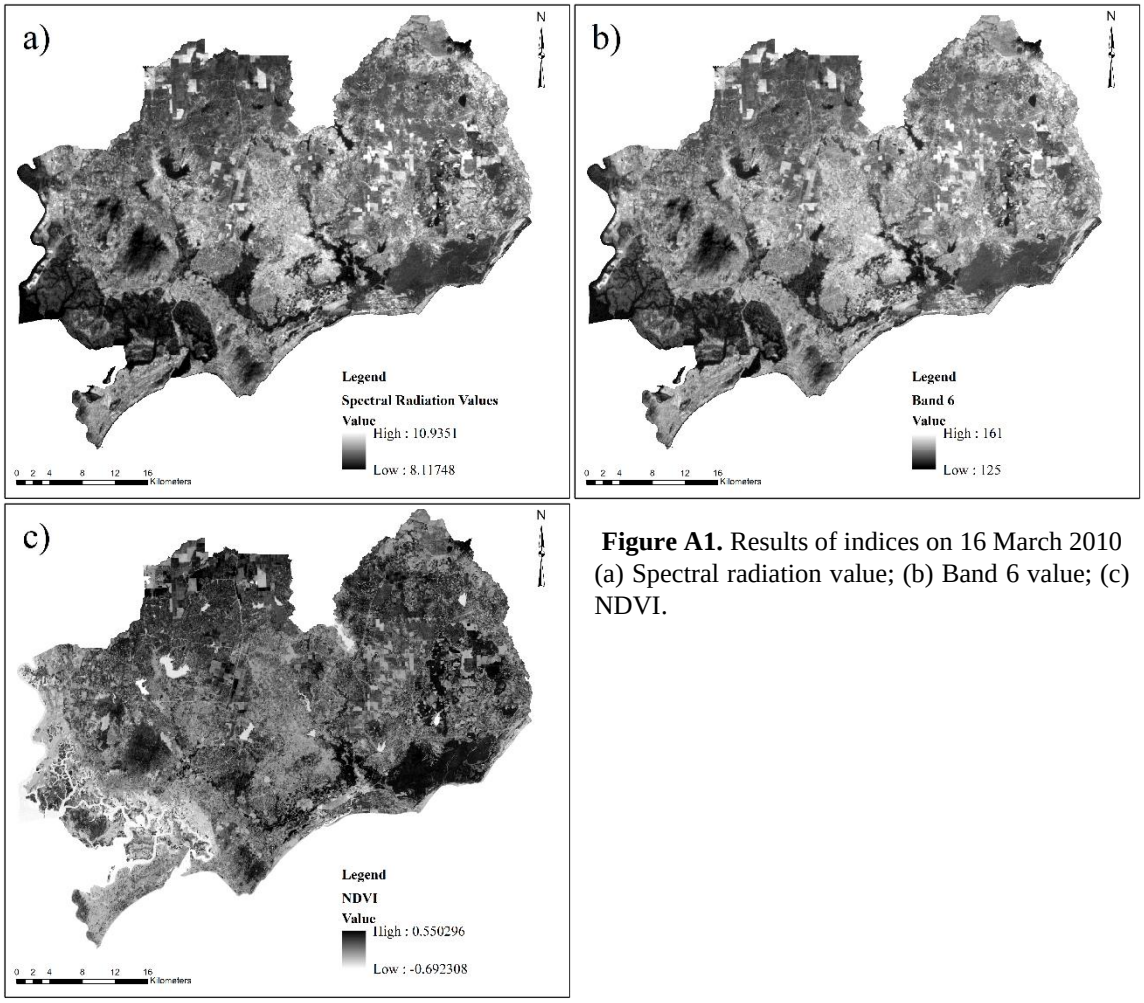

Figure A1. Results of indices on 16 March 2010 (a) Spectral radiation value; (b) Band 6 value; (c) NDVI.

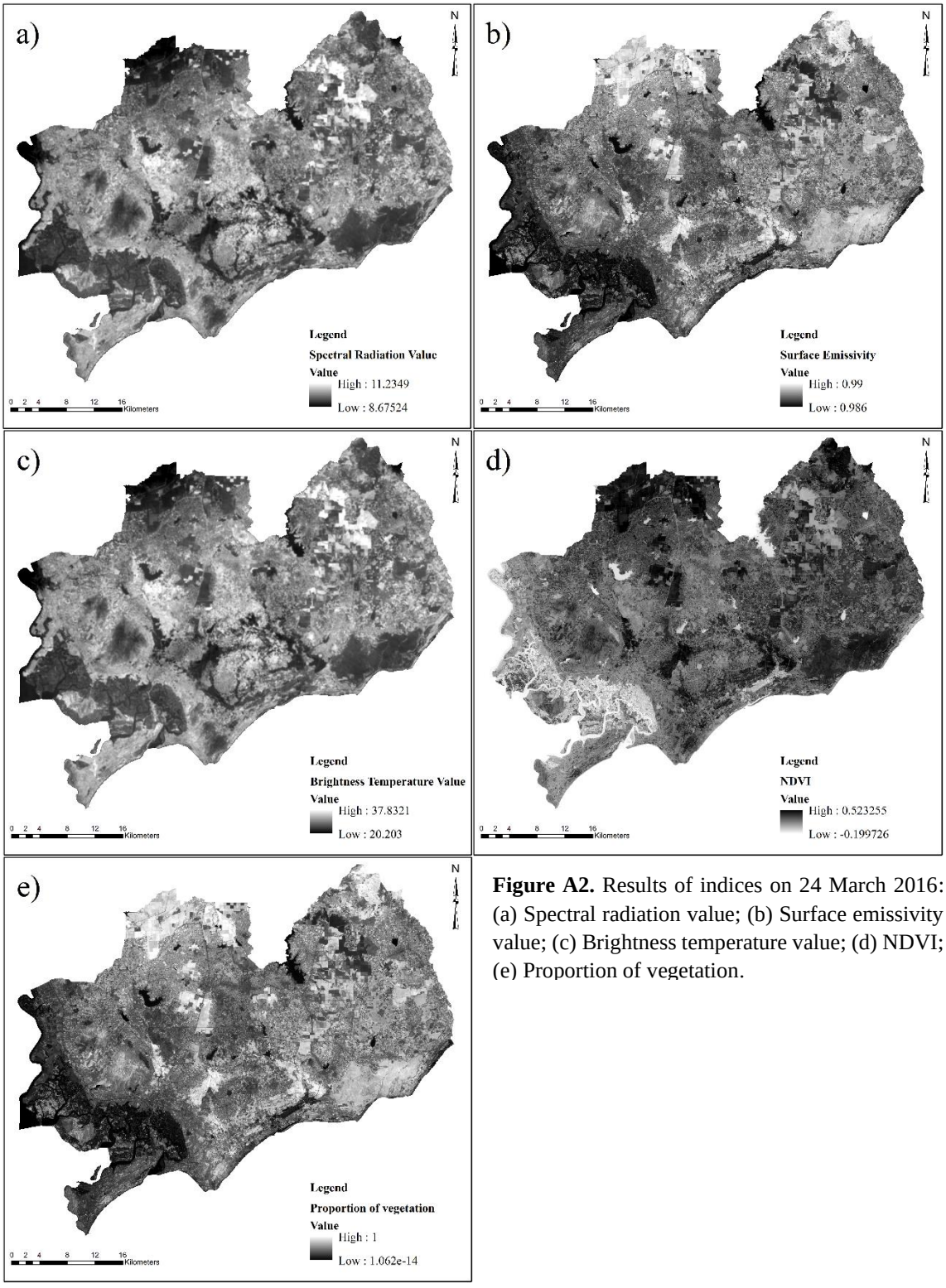

Figure A2. Results of indices on 24 March 2016: (a) Spectral radiation value; (b) Surface emissivity value; (c) Brightness temperature value; (d) NDVI; (e) Proportion of vegetation.

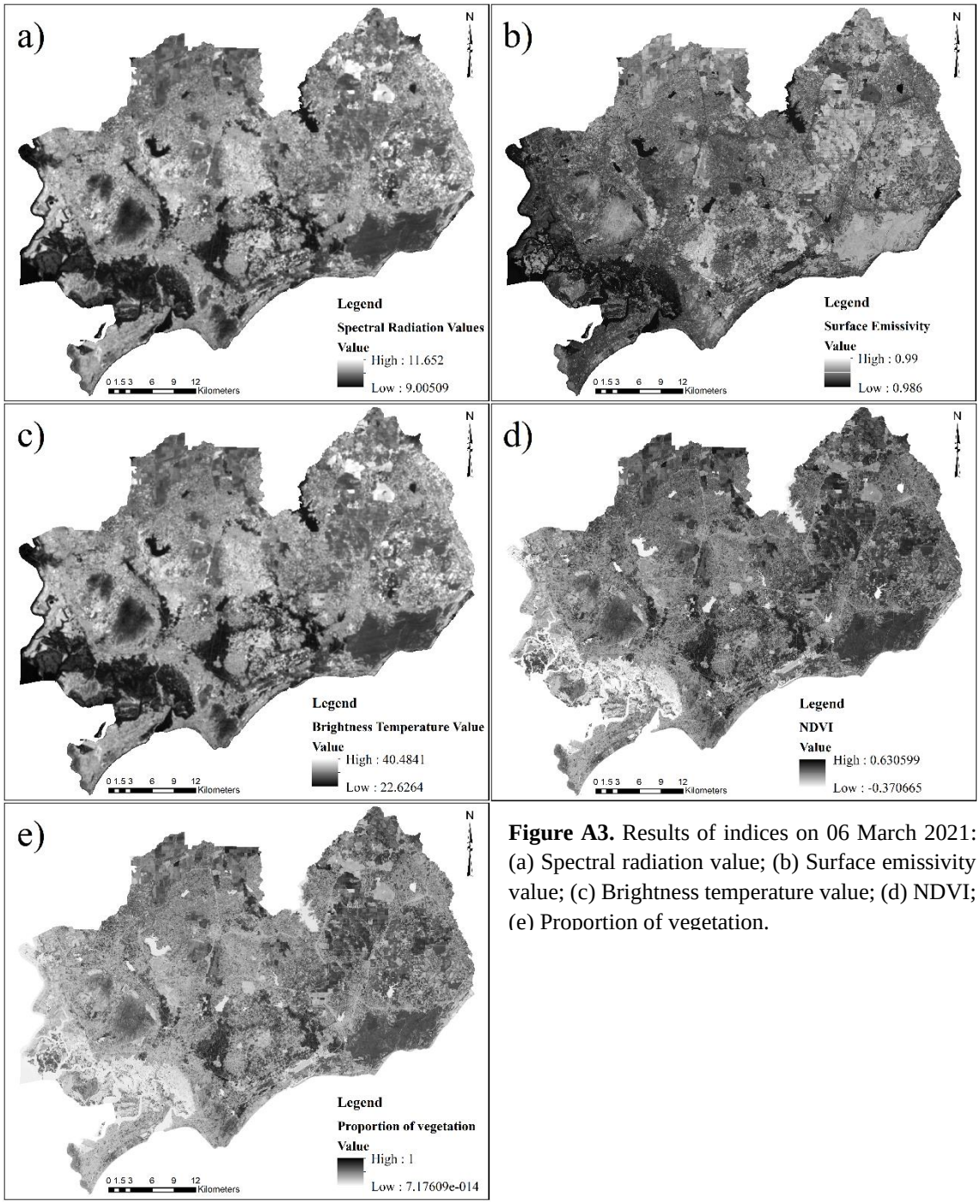

Figure A3. Results of indices on 06 March 2021: (a) Spectral radiation value; (b) Surface emissivity value; (c) Brightness temperature value; (d) NDVI; (e) Proportion of vegetation.